

Manganese deficiency alters high-density lipoprotein subclass structure in the sprague-dawley rat

Paul N. Taylor, Howard H. Patterson,* and Dorothy J. Klimis-Tavantzis

Department of Food Science and Human Nutrition; and *Department of Chemistry, University of Maine, Orono, ME USA

Dietary manganese affects lipid and lipoprotein metabolism. In the Sprague-Dawley rat, manganese deficiency affects high-density lipoprotein composition and may alter lipoprotein structural stability. This study assessed the effects of manganese on high-density lipoprotein subclass structure, dynamics, and mobility, using fluorescence quenching and fluorescence polarization techniques. Male Sprague-Dawley rats were fed diets deficient or adequate in manganese. High-density lipoprotein₁ (HDL₁, density 1.05 to 1.077 kilograms/liter) and high-density lipoprotein₂ (HDL₂, density 1.077 to 1.21 kilograms/liter) were separated by density gradient ultracentrifugation. Iodide quenching of intrinsic (tryptophan) fluorescence showed that there were at least two types of fluorophores in both lipoprotein subclasses. Differences in dynamics and accessibility were noted in HDL₁ (deficient, $K_{sv} = 16.9 \text{ (mol/L)}^{-1}$, $f_a = 20\%$; adequate, $K_{sv} = 9.8 \text{ (mol/L)}^{-1}$, $f_a = 27\%$) and in HDL₂ (deficient, $K_{sv} = 0.89 \text{ (mol/L)}^{-1}$, $f_a = 100\%$; adequate, $K_{sv} = 4.71 \text{ (mol/L)}^{-1}$, $f_a = 36\%$). Differences in polarized fluorescence emission were seen in HDL₂ but not in HDL₁ (deficient, $P = 0.193$; adequate, $P = 0.213$). There were no differences in dynamics, accessibility, or polarized fluorescence in apolipoproteins from either subclass. The data suggest structural changes in HDL₁ and changes in the rotational motion of the proteins in HDL₂. These changes may affect HDL metabolism in the rat. (J. Nutr. Biochem. 7:392–396, 1996.)

Keywords: manganese; HDL₁; HDL₂; fluorescence quenching; fluorescence polarization

Introduction

Manganese deficiency in Sprague-Dawley rats affects high density lipoprotein (HDL) composition^{1–3} and may alter lipoprotein structural stability.³ Consequences of these effects may include altered receptor recognition and catabolism of HDL, ultimately affecting cholesterol metabolism.

HDLs are a heterogenous group of particles that may be separated into two or more discrete subclasses of characteristic size, density, and composition.⁴ Researchers using fluorescence spectroscopy to assess HDL structure and dynamics in the past have focused on total HDL, i.e., those particles of density 1.05 to 1.21 kg/L.^{3,5–7} We isolated by density gradient ultracentrifugation two distinct subclasses

of HDL from Sprague-Dawley rats, HDL₁ (density 1.05 to 1.077 kg/L) and HDL₂ (density 1.077 to 1.21 kg/L).^{8,9}

Our objective was to assess the effects of manganese on HDL subclass structure, dynamics and mobility, using fluorescence spectroscopy. For macromolecules such as proteins, fluorescence measurements can provide information about conformation, flexibility, and rotational diffusion.¹⁰ Fluorescence quenching, a process where the fluorescence intensity of a protein is decreased through interaction with a quencher, provides information about the accessibility of the fluorophore to the quencher, the diffusion rate of the quencher, and the localization of the fluorophore(s) in the protein.¹¹ For the experiments described here, the intrinsic fluorescence (that due to fluorophores naturally a part of the proteins) of HDL₁, HDL₂, apoHDL₁, and apoHDL₂ was quenched by iodide and acrylamide to determine the accessibility of their tryptophan residues. Fluorescence polarization is determined by exciting a sample with polarized light and measuring the extent of depolarization of the fluores-

Address reprint requests to Dr. D.J. Klimis-Tavantzis at the University of Maine, 20 Merrill Hall, Orono, ME 04469-5749 USA
Received July 19, 1995; April 3, 1996.

cence emission. The most important factors determining the extent of depolarization are the motion of the protein and energy transfers between like chromophores. Therefore, the utility of the technique lies in the ability to detect changes in the mobility of either the entire protein molecule or of some part of it.¹⁰ We used polarized fluorescence measurements during quenching by iodide and acrylamide to provide information about the surface and interior mobility of the native proteins and the apolipoproteins.

Methods and materials

Animals and diets

Weanling male Sprague-Dawley rats, average body weight 41 g (Charles River Laboratories, Wilmington, MA, USA), were randomly assigned to either a manganese-deficient (MnD, 0.48 mg/kg) or a manganese-adequate (MnA, 90 mg/kg) diet. Both diets contained 691 g/kg dextrose, 200 g/kg egg white solids, and 4 g/kg D-L methionine (Tekland Test Diets, Madison, WI, USA), 60 g/kg corn oil ("Mazola," Best Foods, Englewood Cliffs, NJ, USA), 10 g/kg vitamin mix (A.O.A.C. Special Vitamin Mixture, U.S. Biochemical Corp., Cleveland, OH, USA), 2 mg/kg biotin (Harlan Sprague-Dawley, Madison, WI, USA), and a trace mineral mix (ICN Biochemicals, Cleveland, OH, USA) containing 121.5 g/kg glucose without manganese carbonate (MnD) or 115.5 g/kg glucose and 6.02 g/kg manganese carbonate (MnA). The animals were allowed free access to food and water for 15 weeks. The rats were housed in individual stainless steel mesh-bottomed cages in a temperature-controlled room (22°C) with a dark period from 1800 hr to 0600 hr. The rats were weighed weekly.

Blood and tissue sampling

At the end of the 15-week feeding period, food was withheld overnight. All animals were anesthetized with diethyl ether and after laparotomy, blood was withdrawn by cardiac puncture into syringes containing Na₂EDTA (1 g/L of blood). Plasma was separated by low speed centrifugation, preservatives were added and aliquots were frozen (-80°C) for later biochemical analyses. Livers were removed and weighed, frozen (-80°C), lyophilized, and pulverized. Liver manganese was determined by the Maine Forest and Agricultural Experiment Station Analytical Laboratory using atomic absorption spectroscopy.

Lipoprotein isolation and delipidation

Lipoproteins were separated by a single-step density gradient ultracentrifugation, using Sudan black in DMSO to stain the lipoproteins.⁹ The dye does not interfere with fluorescence analysis except for slightly diminished fluorescence intensity.^a The VLDL (<1.006 kg/L) and the LDL (1.006 to 1.05 kg/L) were aspirated and not used. The HDL₁ (1.05 to 1.077 kg/L) and HDL₂ (1.077 to 1.21 kg/L) were recovered by tube slicing and aspiration, then dialyzed 48 hr against six volumes of cold (4°C) saline (150 mmol/L NaCl, 0.05% Na₂EDTA, pH 7). Homogeneity of the subclasses was assessed by agarose gel electrophoresis¹² using a commercial kit (Princeton Separations, Freehold, NJ, USA). Aliquots of the native particles were frozen (-80°C) for later analyses.

Apolipoproteins were obtained by delipidating the native particles with methanol and diethyl ether as described by Herbert et al.¹³ and modified by Osborne.¹⁴ The recovered protein was re-

solubilized in 10 mmol/L Tris, 100 mmol/L NaCl, 1 mmol/L Na₂N₃, 1 mmol/L Na₂EDTA, 2 mol/L guanidium HCl, pH 7.4,¹⁴ then dialyzed against a phosphate-buffered saline (PBS; KH₂PO₄:Na₂HPO₄, 1:4.08, pH 7.4).

Fluorescence quenching

Native lipoproteins were thawed to 22°C in a water bath, then dialyzed against PBS. The HDL₁, HDL₂, and apoHDL₂ were diluted with PBS to 20 mg/L, and the apoHDL₁ were diluted to 10 mg/L, to reduce inner filtering effects ($A_{280} < 0.05$).¹⁵

Spectra were generated on a Perkin-Elmer MPF-4 spectrofluorimeter equipped with a Hamamatsu R928 photomultiplier tube detector and a 150-watt Xenon lamp, with data output to a Perkin-Elmer 56 chart recorder. The excitation and emission maxima were recorded for each class of sample.

Two quenching solutions were used. One was a charged quencher, 1 mol/L KI in PBS (1 mmol/L K₂S₂O₃ was added to prevent I₃⁻ formation). Acrylamide (2 mol/L in PBS) was used as a neutral quencher. Buffers and quenchers were dispensed into test tubes, vortexed, and allowed to equilibrate for 12 hr. Potassium chloride (1 mol/L in PBS) was added as necessary to the iodide tubes, and PBS was added as necessary to the acrylamide tubes, to maintain ionic strength and to standardize the volume so that it was not necessary to correct for dilution. After equilibrating, samples were added to each tube, vortexed, and allowed to equilibrate for 1 hour. The final protein concentrations were 10 mg/L (HDL₁, HDL₂, apoHDL₂) and 5 mg/L (apoHDL₁). Experiments were done at 22°C.

The contents of each test tube were carefully transferred (to avoid quenching by oxygen) to a 1 cm pathlength quartz microcuvet. The excitation wavelength was always 295 nm, whereas the emission intensity was monitored at 338 nm for HDL₁ and HDL₂ and 353 nm for apoHDL₁ and apoHDL₂. Excitation and emission slit widths were equal, 4, 4.5, or 5 nm to maximize the intensity of the individual samples. Dynode potential was 800 volts and the coarse sensitivity (signal amplification) was 3 units for full-scale standardization of the chart recorder with 1 µg/L quinine sulfate in 0.05 mol/L H₂SO₄. The intensity of a buffer blank was subtracted from each measured intensity. Between each intensity measurement the excitation radiation was shuttered and the emission light-path was blocked. With acrylamide quenching, the data were corrected¹⁶ for the optical absorbance of acrylamide at 295 nm.

Quenching constants for iodide and acrylamide for apoHDL₁ and apoHDL₂ were calculated using the Stern-Volmer¹⁷ equation:

$$F_0/F = 1 + k_q\tau_0[Q] = 1 + K_{SV}[Q] \quad (1)$$

where F_0 and F are the fluorescence intensities recorded in the absence and presence, respectively, of the quencher Q , k_q is a bimolecular quenching constant, τ_0 is the lifetime of the fluorophore in the absence of Q , and $K_{SV} = k_q\tau_0$ is the Stern-Volmer quenching constant.¹¹ The data were plotted as F_0/F versus $[Q]$, and from these linear plots the K_{SV} were taken from the slopes of the best-fit lines to the plotted data. For native HDL₁ and HDL₂ particles the iodide Stern-Volmer plots were not linear, but curved downward. Therefore, iodide quenching constants were calculated from modified Stern-Volmer (reciprocal) plots, $F_0/(F_0 - F)$ versus $1/[Q]$, to provide a linear fit. From the modified plot, K_{SV} was calculated from the slope of the best-fit line, $m = 1/f_a K_{SV}$, where f_a represents the accessible portion of two or more unequally accessible classes of fluorophores, and may be calculated from the intercept of the best-fit line, $b = 1/f_a$.^{3,11,18}

Polarized fluorescence

Samples were prepared as described above. The excitation and emission slit widths for all experiments were equal, 13.25 nm. The

^a Unpublished data.

dynode potential for the photomultiplier/detector was 800 V and the coarse sensitivity was 10 units. A Perkin-Elmer polarizer accessory was used in the MPF-4 spectrofluorimeter to hold Polaroid Polarcoat HN P'B filters in both the excitation and emission lightpaths. Filter integrity was checked with 1 $\mu\text{mol/L}$ rhodamine B in 95% glycerol. The excitation radiation was shuttered and the emission lightpath blocked between each intensity measurement. Polarized fluorescence was assessed at iodide concentrations of 0, 0.045, 0.09, 0.135, and 0.2 mol/L, and at acrylamide concentrations of 0, 0.1, 0.2, 0.3, and 0.4 mol/L. Four intensities (two vertically polarized, V_{em} and V_{ex} , and two horizontally polarized, H_{em} and H_{ex}) were measured from the blank and from the sample containing protein only (no quencher). Two were used to compute a correction factor for the emission monochromator, $G = V_{ex}/H_{ex}$.¹⁹ Only H_{ex} and V_{em} were measured for the remaining tubes, and the polarized fluorescence was computed using the following equation:

$$P = (V_{em} - GH_{ex}) / (V_{em} + GH_{ex})$$

Polarized fluorescence data collected during iodide quenching were interpreted as an indication of the surface mobility of the proteins, whereas polarized fluorescence data collected during acrylamide quenching were interpreted as an indication of the combined surface and internal mobility of the proteins.

Statistical analysis

Data are expressed as means \pm SEM. Student's two-tailed *t*-test was used to assess differences between groups. The significance level was $P \leq 0.05$.

Results

Both groups of rats gained weight during the 15-week period. However, BW differences between the two groups (MnD, $n = 21$; MnA, $n = 20$) were significant ($P \leq 0.05$) by the third week and continued to the 15th week, when the mean final weights were 429 ± 8 g for MnD rats and 500 ± 10 g for MnA rats ($P = 0.0001$). The liver weights of the MnD rats (11 ± 0.3 g) were significantly different from ($P = 0.0004$) the MnA rats (13 ± 0.3 g), but when expressed as a percentage of the final BW there was no difference (3%, both groups). The manganese deficiency status of MnD rats was confirmed by the liver manganese assays. Mean liver manganese was 2.13 ± 0.078 mg/kg in MnD rats and 8.80 ± 0.15 mg/kg in MnA rats ($P = 0.0001$).

Conventional fluorescence scans showed emission maxima of 338–340 nm for the native HDL₁ and HDL₂ when excited at 280, 290, and 295 nm. The emission maxima of the apoHDL₁ and apoHDL₂ were 353–356 nm when excited at 280 or 290 nm, but shifted to 333 to 340 nm with a broad shoulder at 353 nm when excited at 295 nm. This phenomenon was attributed to emission from tyrosinate, which can form a complex with the phosphate in the buffer,¹¹ and confirmed that the proteins were completely unfolded by the delipidation process.

Iodide quenching (Stern-Volmer) plots of intrinsic tryptophan fluorescence in native HDL₁ (Figure 1a) and native HDL₂ (not shown) curved toward the x-axis, indicating the presence of at least two classes of fluorophores of differing accessibility to the quencher. A modified Stern-Volmer plot (Figure 1b) showed that the tryptophan residues of the MnD and MnA HDL₁ differed in dynamics (MnD, $K_{sv} = 16.9$

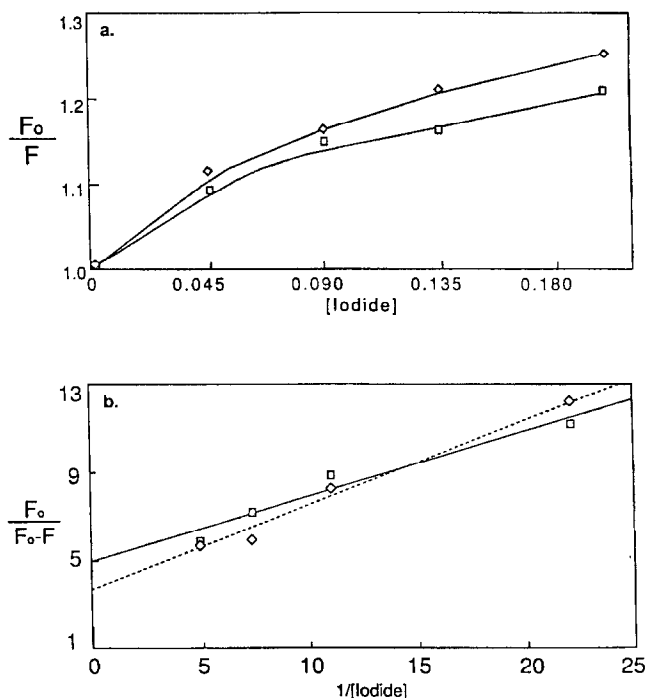


Figure 1 a) Stern-Volmer fluorescence quenching plots of HDL₁ in MnD, $n = 6$ (\diamond) and MnA, $n = 8$ (\square) rats and b) modified Stern-Volmer fluorescence quenching plots of HDL₁ in MnD ($y = 0.292x + 4.933$, $r^2 = 0.95$, $K_{sv} = 16.9$ (mol/L)⁻¹) and MnA ($y = 0.379x + 3.695$, $r^2 = 0.98$, $K_{sv} = 9.8$ (mol/L)⁻¹) rats.

(mol/L)⁻¹; MnA, $K_{sv} = 9.8$ (mol/L)⁻¹) as well as accessibility (MnD, $f_a = 20\%$ and MnA, $f_a = 27\%$). The modified plot for the HDL₂ (not shown) also showed differences in dynamics and accessibility for those particles (MnD, $K_{sv} = 0.89$ (mol/L)⁻¹, $f_a = 100\%$; MnA, $K_{sv} = 4.7$ ((mol/L)⁻¹, $f_a = 36\%$). All of the tryptophan residues of MnD and MnA apoHDL₁ and apoHDL₂ were accessible to iodide, with equivalent dynamics (apoHDL₁:MnD 2.40 and MnA 2.60 (mol/L)⁻¹; apoHDL₂:MnD 3.06 and MnA 3.22 (mol/L)⁻¹). The acrylamide quenching parameters were equivalent for HDL₁ (MnD 2.11 and MnA 2.23 (mol/L)⁻¹), apoHDL₁ (MnD 4.94 and MnA 4.26 (mol/L)⁻¹), HDL₂ (MnD 2.14 and MnA 2.14 (mol/L)⁻¹) and apoHDL₂ (MnD 8.68 and MnA 8.20 (mol/L)⁻¹).

Polarized fluorescence, P , was measured for each sample before the addition of the quencher and at each step in the subsequent titrations. The polarized fluorescence of MnD HDL₂ ($P = 0.193 \pm 0.008$) was different ($P = 0.08$) from that of MnA HDL₂ ($P = 0.213 \pm 0.006$) before either quencher was added.

Polarized fluorescence values determined during iodide quenching revealed little difference (HDL₁, $P = 0.53$ to 0.83 ; apoHDL₁, $P = 0.54$ to 0.79) in rotational motion between MnD and MnA native HDL₁ and apoHDL₁, and $P_{MnD} > P_{MnA}$. However, when MnD and MnA native HDL₂ and apoHDL₂ were compared, the MnD samples exhibited greater rotational motion in the presence of iodide, the differences were greater (HDL₂, $P = 0.08$ to 0.35 ; apoHDL₂, $P = 0.08$ to 0.51), and $P_{MnD} < P_{MnA}$.

Polarized fluorescence values determined during acryl-

amide quenching showed that the MnD native HDL₂ exhibited very pronounced differences in rotational motion when compared to the MnA HDL₂ (Figure 2). The native MnD and MnA HDL₁ were not different ($P = 0.57$ to 0.99) and the apoHDL₁ were not different ($P = 0.69$ to 0.95), and $P_{\text{MnD}} > P_{\text{MnA}}$. Likewise, the apoHDL₂ were not different ($P = 0.23$ to 0.92) and $P_{\text{MnD}} < P_{\text{MnA}}$.

Discussion

The manganese-deficient diet retarded the growth of the MnD rats. Boyer et al.²⁰ observed that feeding rats a manganese-deficient diet results in marked growth retardation. Studies where no significant effect of manganese deficiency on growth is seen are typically of short duration^{1,2,21-23} or were done before the advent of modern analytical techniques and purified diets.^{23,24} One possible explanation is that in the rat, bone stores of manganese are mobilized in the early weeks of feeding a manganese-deficient diet, making it difficult to induce deficiency by diet within a short time period.²⁵ The retarded-growth effect associated with manganese deficiency in murine models is not a function of reduced food intake, rather it is a result of reduced efficiency of food conversion in the manganese-deficient animals.^{20,26,27} Neither free-feeding protocols nor pair-feeding protocols have shown any significant difference in the amount of food consumed by animals fed manganese-deficient, manganese-adequate or manganese-supplemented diets,^{1,2,20,22,24,28} regardless of experiment duration. Our 15-week feeding period was chosen to optimize the development of manganese deficiency symptoms.

High density lipoproteins are defined as a major class of plasma lipoproteins comprised of two discrete subclasses, one larger, more buoyant and enriched in cholesterol esters, the other smaller, denser, and protein-enriched.^{4,29,30} The HDL as a class of particles undergo significant interconversions, particularly from small, dense particles to large, buoyant particles.²⁹ These interconversions are strongly dependent on the functioning of the enzymes lipoprotein lipase (LPL) and lecithin:cholesterol acyl transferase (LCAT). In turn, LPL requires apoC as a cofactor and LCAT is activated by apoA-I.

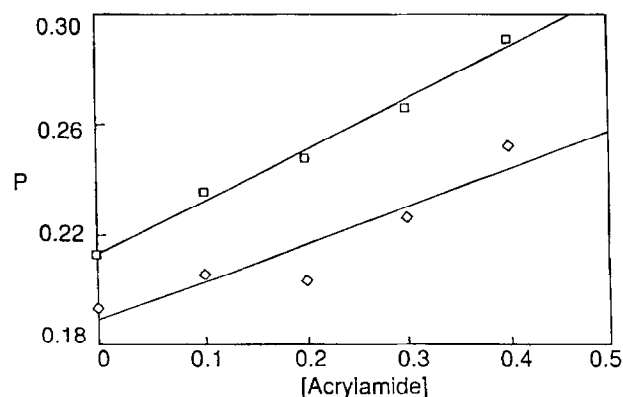


Figure 2 Polarized fluorescence during acrylamide quenching of native HDL₂ from MnD, $n = 6$ (\diamond) and MnA, $n = 8$ (\square) rats. Linear regression parameters are MnD, $y = 0.142x + 0.188$, $r^2 = 0.88$, and MnA, $y = 0.189x + 0.213$, $r^2 = 0.99$.

The effects of murine manganese deficiency on lipoproteins depends on the strain and sex of the animal model and on the time allowed for the deficiency to develop and for clinical signs to manifest. Serum and HDL cholesterol are not significantly affected in Wistar and genetically hypercholesterolemic (RICO) rats fed diets containing 0.12 mg/kg manganese for 8 and 12 weeks, respectively.²¹ Sprague-Dawley and Wistar rats fed diets containing 1 mg/kg manganese for 10 weeks have plasma cholesterol levels equal to or less than, respectively, their littermates receiving 45 mg/kg manganese.¹ However, there are significantly lower plasma apoE, HDL-protein and HDL-cholesterol levels and the HDL protein:cholesterol ratio is elevated in both manganese-deficient strains, while in the manganese-deficient Sprague-Dawley rats there are significantly higher plasma apoA-I and apoA-IV, and HDL-apoC levels, a significantly lower HDL-apoE level, and smaller HDL particles.¹ These changes suggest that HDL metabolism is altered with manganese deficiency and is especially evident in the Sprague-Dawley strain. Davis et al.² and Klimis-Tavantzis et al.³ corroborate these findings in Sprague-Dawley rats, suggesting that these changes result from decreased cholesterol synthesis and/or secretion² or from a change in the structure of the HDL particle.³ Klimis-Tavantzis et al.³ conclude that structural alterations of the native lipoproteins or the apolipoproteins may adversely affect the metabolism of HDL and may ultimately affect the transport and metabolism of cholesterol.

From the differences in dynamics and accessibility (represented by K_{sv} and f_a) and from the polarized fluorescence (P) we can postulate that dietary manganese deficiency altered the structure of the native HDL₁ particles and altered the rotational motion of the HDL₂ proteins, respectively. In the native MnD HDL₁ fewer tryptophan residues were exposed to the anionic quencher iodide, and the iodide was much less efficient at quenching those residues.

Manganese-deficient HDL have more apoA-I relative to the other major apolipoproteins when compared with MnA HDL,¹ which could account for the differences we noted during iodide quenching of HDL₁.^b Therefore, we believe that the MnD HDL₁ particle had an altered protein configuration compared with MnA HDL₁, which may affect its recognition and uptake by the apo B,E receptor in the liver and ultimately affect cholesterol transport.

The native HDL₂ particles from MnD and MnA rats were markedly different in their response to quenching by iodide. All of the tryptophan residues of MnD HDL₂ were exposed to iodide, and the quenching constant was low compared with that for MnA HDL₂, indicating greater efficiency of quenching. Without the evidence from the polarized fluorescence experiments, we might have attributed the differences in dynamics and accessibility to a structural difference in the MnD HDL₂ compared with the MnA HDL₂. When the initial polarized fluorescence values were compared, however, a difference was noted that we believe reflects the rotational motion of the constituent proteins of the

^b Kawano et al.¹ report more apoA-I in MnD Sprague-Dawley rat HDL of density 1.050–1.1963 kg/L, a range which includes HDL₁ and a portion of HDL₂.

MnD and MnA HDL₂ particles. The difference remained throughout the titration of acrylamide and to a lesser extent throughout the titration of iodide. We suggest that greater rotational motion of the MnD HDL₂ proteins might allow a closer approach for the anion to the tryptophan residues. Because manganese "bridges" the anionic groups of glycosaminoglycans with amino acid residues and phospholipids on the surface of lipoproteins,³¹ we surmised that a lack of manganese bridges in the overall lipoprotein surface structure allowed greater rotational motion of the proteins in the MnD HDL₂ particle.

All of the fluorescence quenching and polarized fluorescence data collected for the MnD and MnA apolipoproteins from the two HDL subclasses indicated that there were no fundamental differences in the proteins that could be attributed to the presence or absence of manganese. Rather, these data support the conclusion that the differences are in the native lipoproteins in the interrelationships between the lipid, protein, and phospholipid moieties.

We conclude that manganese deficiency in the Sprague-Dawley rat alters the structure of HDL₁ and alters the rotational motion of the HDL₂ proteins. These changes may have a profound effect on the metabolism and transport of cholesterol in the rat.

Acknowledgments

This work was supported in part by a grant (No. 9407791S) from the American Heart Association, Maine Affiliate. P.N. Taylor (present address: The Jackson Laboratory, 600 Main Street, Bar Harbor, ME 04609-1500 USA) received a summer research fellowship from the American Heart Association, Maine Affiliate and grants from the Association of Graduate Students, University of Maine

References

- Kawano, J., Ney, D.M., Keen, C.L., and Schneeman, B.O. (1987). Altered high density lipoprotein composition in manganese-deficient Sprague-Dawley and Wistar rats. *J. Nutr.* **117**, 902-906
- Davis, C.D., Ney, D.M., and Greger, J.L. (1990) Manganese, iron and lipid interactions in rats. *J. Nutr.* **120**, 507-513
- Klimis-Tavantzis, D.J., Taylor, P.N., Lewis, R.A., Flores, A.L., and Patterson, H.H. (1993). Effects of dietary manganese deficiency on high density lipoprotein composition and metabolism in Sprague-Dawley rats. *Nutr. Res.* **13**, 953-968
- Tribble, D.L. and Krauss, R.M. (1993). HDL and coronary artery disease. *Adv. Internal Med.* **38**, 1-29
- Hart, C.J., Leslie, R.B., and Scanu, A.M. (1970). Fluorescence studies of a high density serum lipoprotein. *Chem. Phys. Lipids* **4**, 367-375
- Jonas, A., Hesterberg, L.K., and Drengler, S.M. (1978). Incorporation of excess cholesterol by high density serum lipoproteins. *Biochim. Biophys. Acta* **528**, 47-57
- Stoeffel, W., Salm, K.P., and Langer, M. (1978). A new method for the exchange of lipid classes of human serum high density lipoprotein. *Hoppe-Seyler's Z. Physiol. Chem.* **359**, 1385-1393
- Lusk, L.T., Walker, L.F., DuBien, L.H., and Getz, G.S. (1979). Isolation and partial characterization of high-density lipoprotein HDL₁ from rat plasma by gradient centrifugation. *Biochem. J.* **183**, 83-90
- Mela, D.J., Cohen, R.S., and Kris-Etherton, P.M. (1987). Lipoprotein metabolism in a rat model of diet-induced adiposity. *J. Nutr.* **117**, 1655-1662
- Freifelder, D. (1982). *Physical Biochemistry. Applications to Biochemistry and Molecular Biology*, Second Ed., p. 537-572. W.H. Freeman, San Francisco, CA USA
- Lakowicz, J.R. (1983). *Principles of Fluorescence Spectroscopy*, p. 257-301 and 347-354, Plenum Press, New York, NY USA
- Johansson, B.G. (1972). Agarose gel electrophoresis. *Scand. J. Clin. Lab. Invest.* **29** (Suppl. 124), 7-19
- Herbert P.N., Bausserman, L.L., Henderson, L.O., Heinen, R.J., LaPiana, M.J., Church, E.C., and Shulman, R.S. (1978). Apolipoprotein Quantitation. In *The Lipoprotein Molecule* (H. Peeters, ed.), p. 35-56, Plenum, New York, NY USA
- Osborne, Jr., J.C. (1986). Delipidation of plasma lipoproteins. *Meth. Enzymol.* **128**, 213-222
- Miller, J. (1981). *Standards in Fluorescence Spectrometry*, p. 27, Chapman and Hall, London UK
- MacDonald, B. (1994). *Inner Filter Effects and the Quenching of Pyrene by Dissolved Organic Carbon*, p. 12-30, MS Thesis, University of Maine, Orono, ME USA
- Stern, O. and Volmer, M. (1919). Über die Abklingungszeit der Fluoreszenz. *Phys. Z.* **20**, 183-188
- Lehrer, S.S. (1971). Solute perturbation of protein fluorescence. The quenching of the tryptophan fluorescence of model compounds and of lysozyme by iodide ion. *Biochemistry* **10**, 3254-3263
- Chen, R.F. and Bowman, R.L. (1965). Fluorescence polarization: Measurement with ultraviolet-polarizing filters in a spectrofluorimeter. *Science* **147**, 729-732
- Boyer, P.D., Shaw, J.H., and Phillips, P.H. (1942). Studies on manganese deficiency in the rat. *J. Biol. Chem.* **143**, 417-425
- Klimis-Tavantzis, D.J., Leach, Jr., R.M., and Kris-Etherton, P.M. (1983). The effect of dietary manganese deficiency on cholesterol and lipid metabolism in the Wistar rat and in the genetically hypercholesterolemic RICO rat. *J. Nutr.* **113**, 328-336
- Brock, A.A., Chapman, S.A., Ulman, E.A., and Wu, G. (1994). Dietary manganese deficiency decreases rat hepatic arginase activity. *J. Nutr.* **124**, 340-344
- Orent, E.R. and McCollum, E.V. (1931). Effects of deprivation of manganese in the rat. *J. Biol. Chem.* **92**, 651-678
- Orent, E.R. and McCollum, E.V. (1932). The estrual cycle in rats on a manganese-free diet. *J. Biol. Chem.* **98**, 101-102
- Freeland-Graves, J. and Llanes, C. (1994). Models to study manganese deficiency. In *Manganese in Health and Disease* (D.J. Klimis-Tavantzis, ed.), p. 59-86, CRC Press, Boca Raton, FL USA
- Paynter, D. (1980). Changes in activity of manganese superoxide dismutase enzyme in tissues of the rat with changes in dietary manganese. *J. Nutr.* **110**, 437-447
- Fahim, F.A., Morcos, N.Y.S., and Esmat, A.Y. (1990). Effects of dietary magnesium and/or manganese variables on the growth rate and metabolism of mice. *Ann. Nutr. Metabol.* **34**, 183-192
- Visek, W.J., Prior, R.L., Ulman, E.A., and Mangian, H. (1992). Additive depression of liver arginase by dietary deficiencies of arginine and manganese. *FASEB J.* **6**, A1951
- Eisenberg, S. (1984). High density lipoprotein metabolism. *J. Lipid Res.* **25**, 1017-1058
- Shepherd, J. (1994). Lipoprotein metabolism. An overview. *Drugs* **47** (Suppl. 2), 1-10
- Pifat, G., Udovicic, L., Brnjac-Kraljević, J., Jürgens, G., Holasek, A., and Herak, J.N. (1988). Competitive ion binding to low density lipoproteins: an electron spin resonance study. *Chem. Phys. Lipids* **46**, 99-105